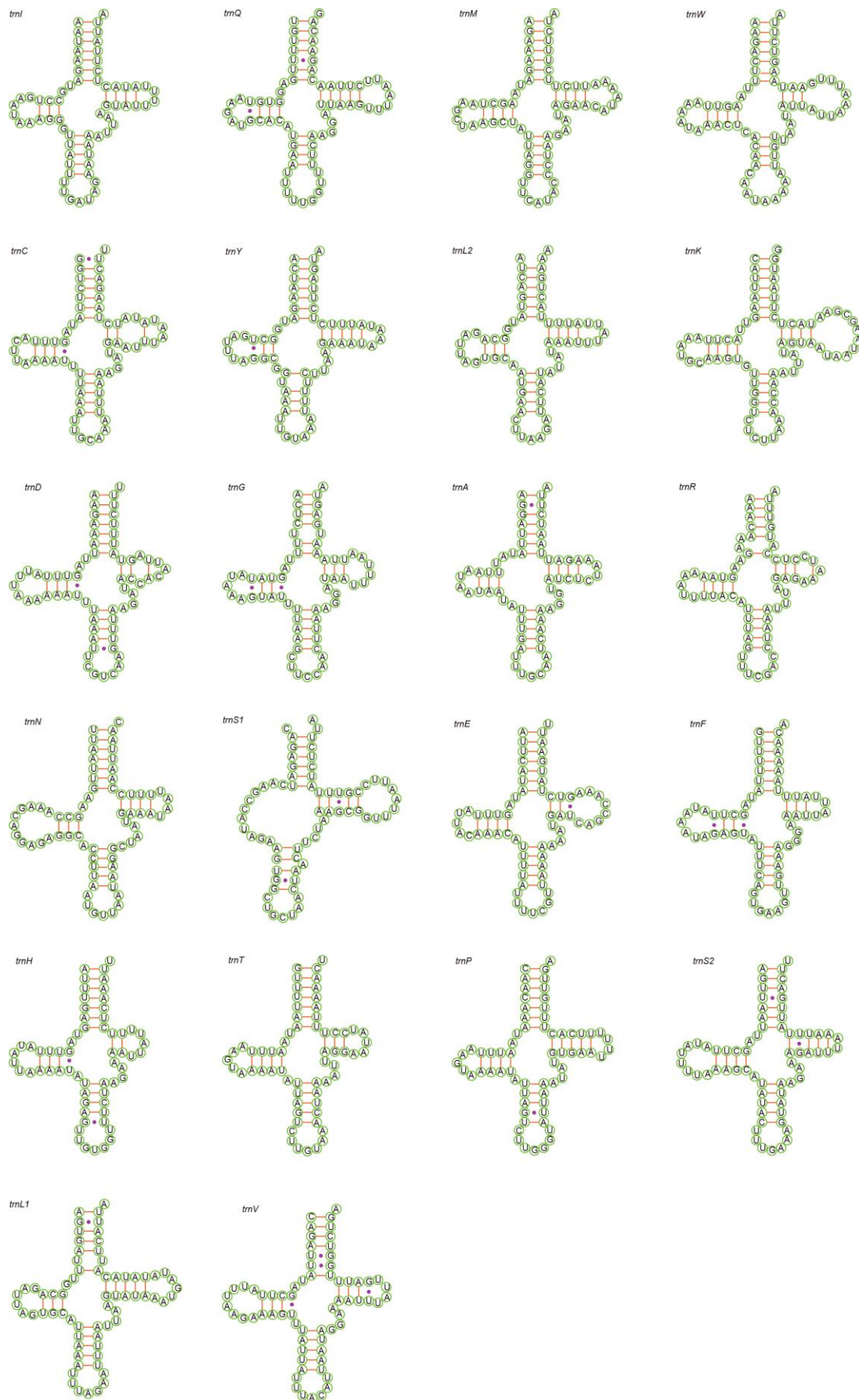
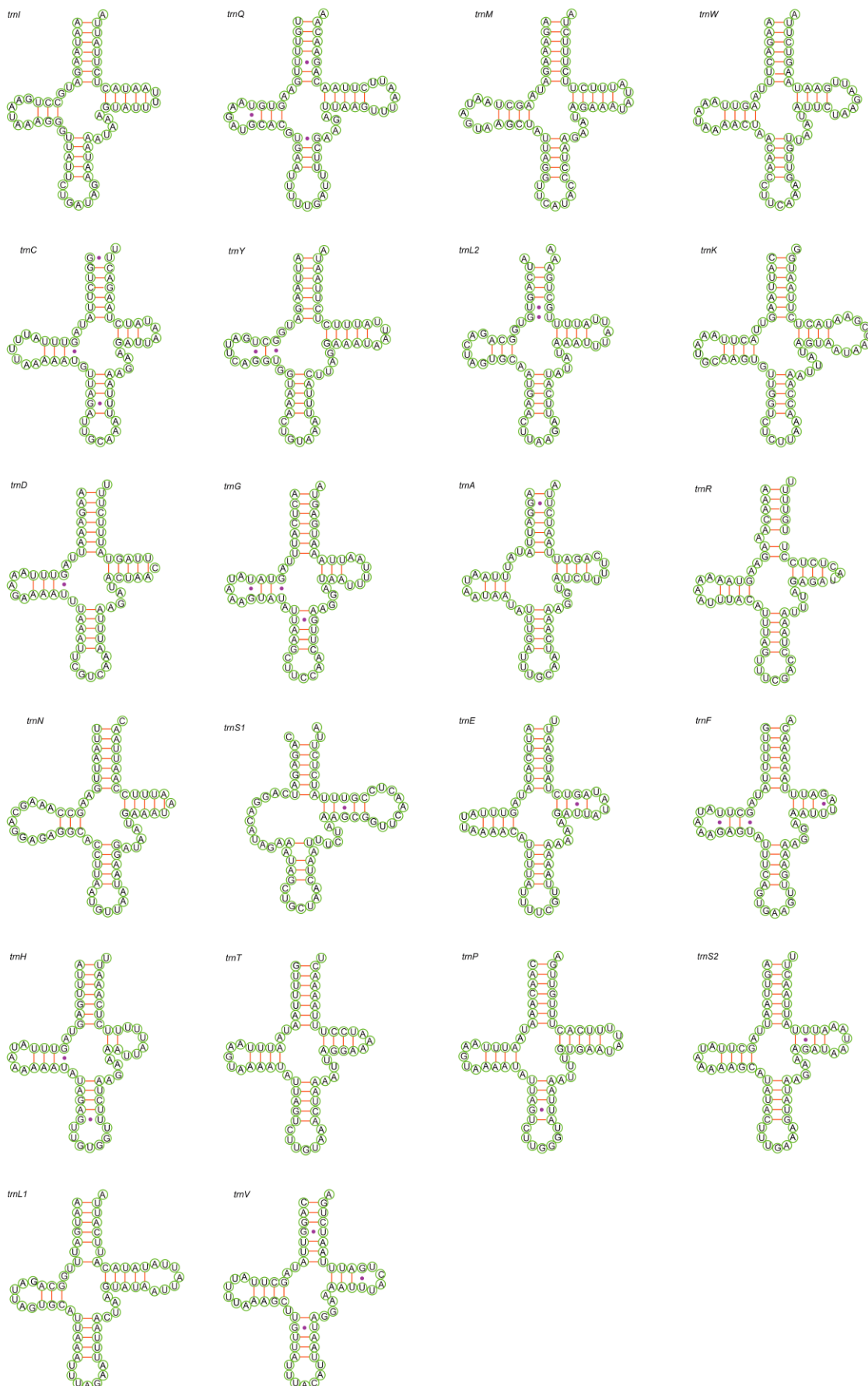


**Figure S1.** Predicted secondary structures of tRNA genes of *Aconurella diplachnis*.



**Figure S2.** Predicted secondary structures of tRNA genes of *Aconurella montana*.



**Figure S3.** Predicted secondary structures of tRNA genes of *Aconurella prolixa*.

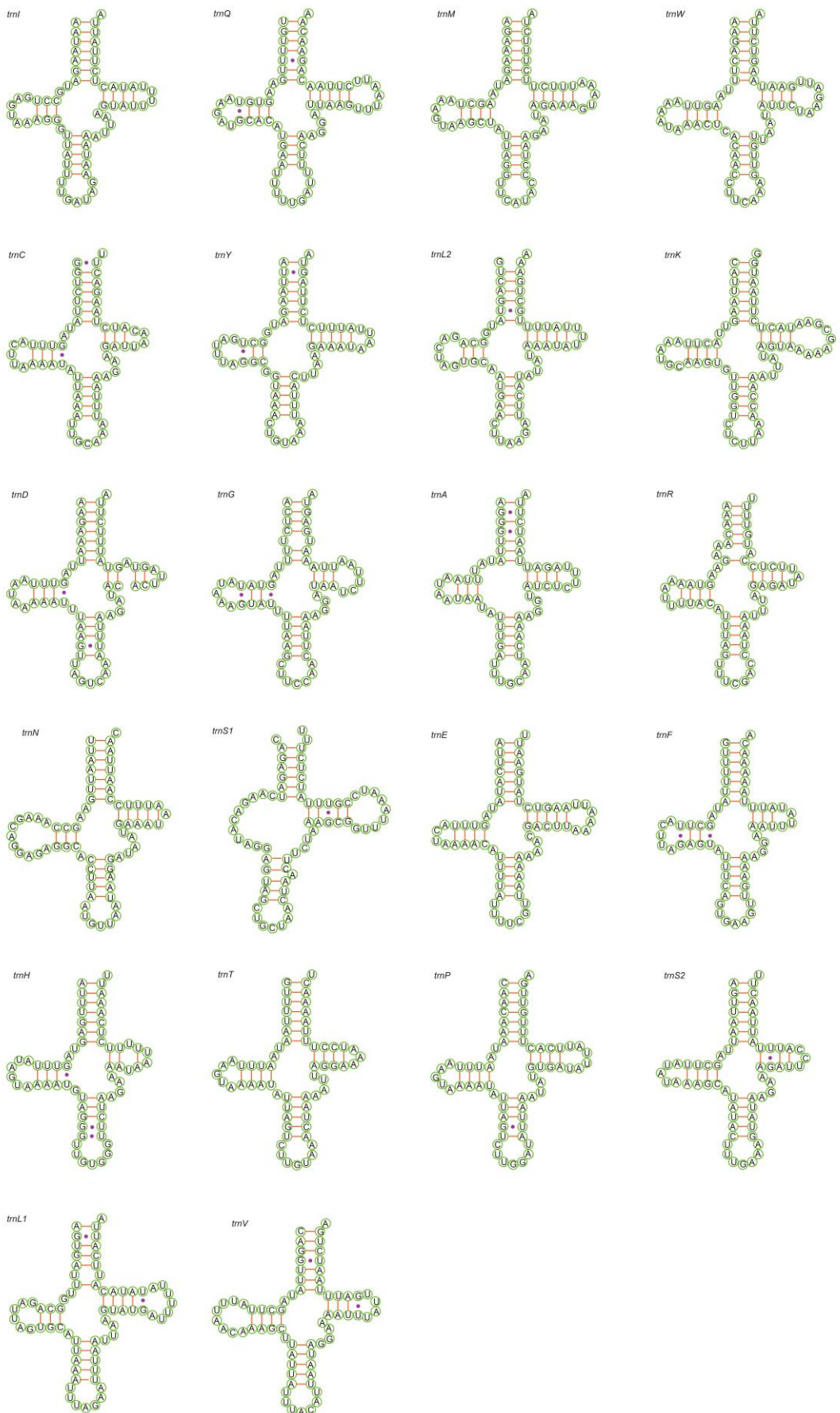


**Figure S4.** Predicted secondary structures of tRNA genes of *Aconurella sibirica*.

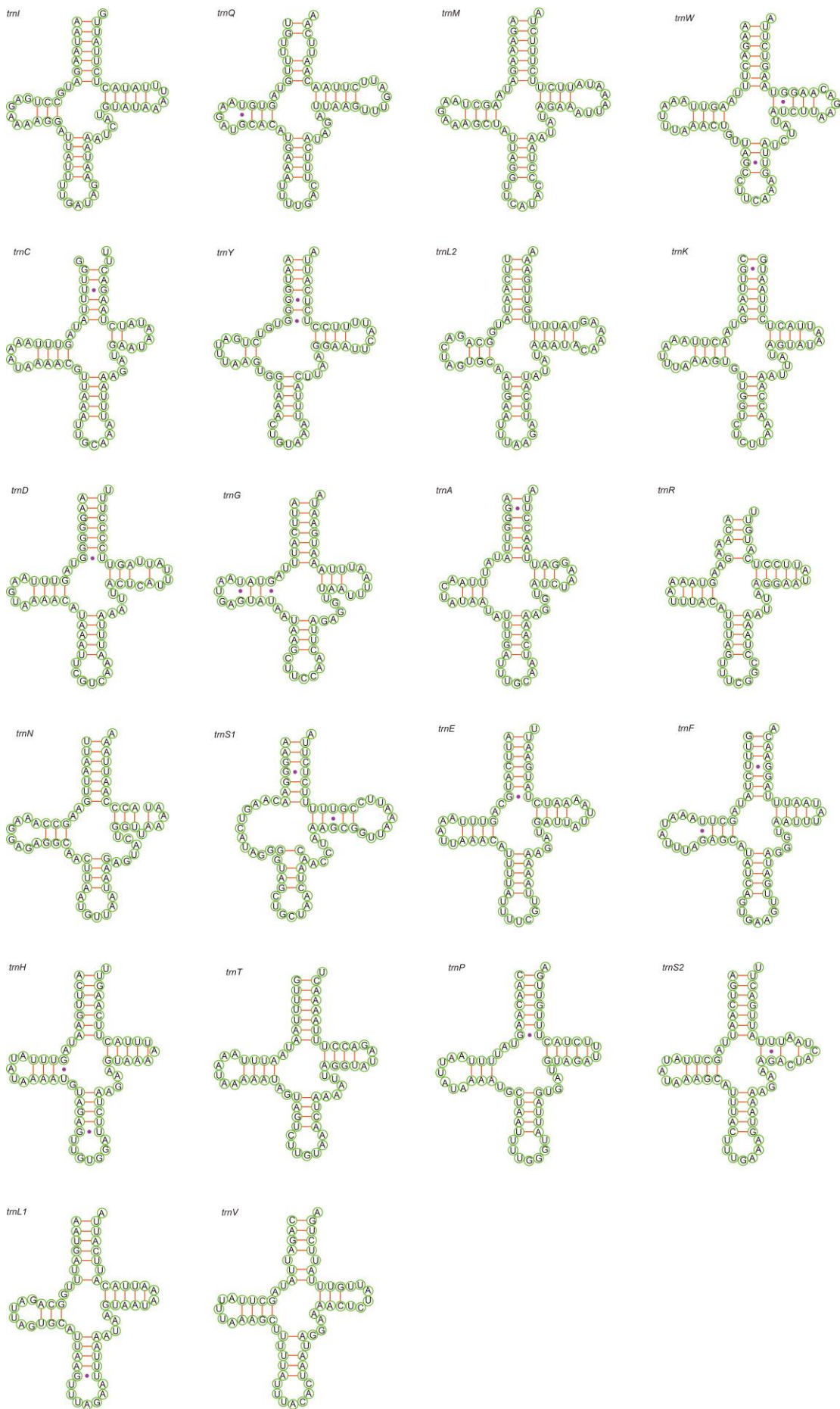


**Figure S5.** Predicted secondary structures of tRNA genes of *Exitianus nanus*.

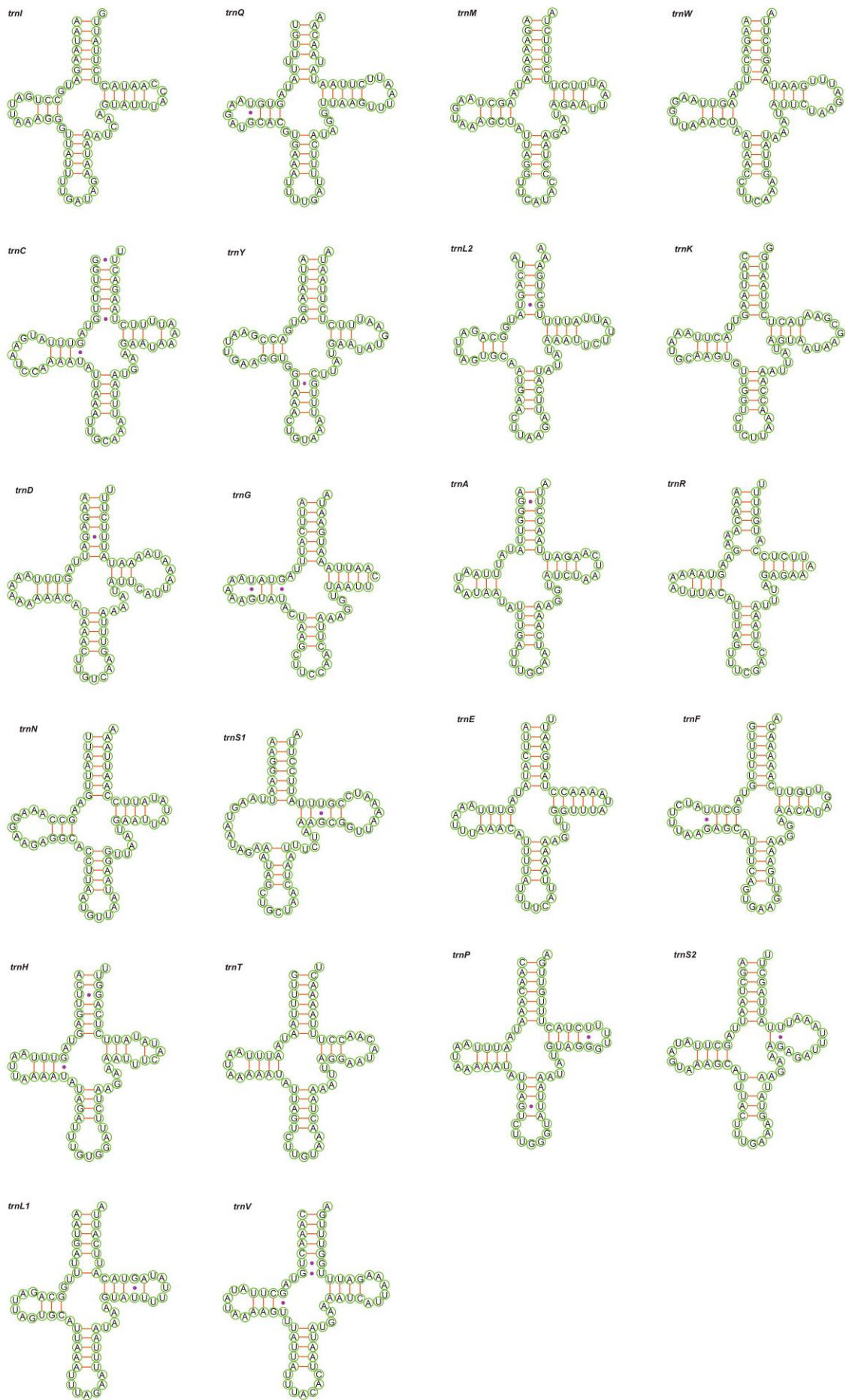


**Figure S6.** Predicted secondary structures of tRNA genes of *Doratura stylata*.

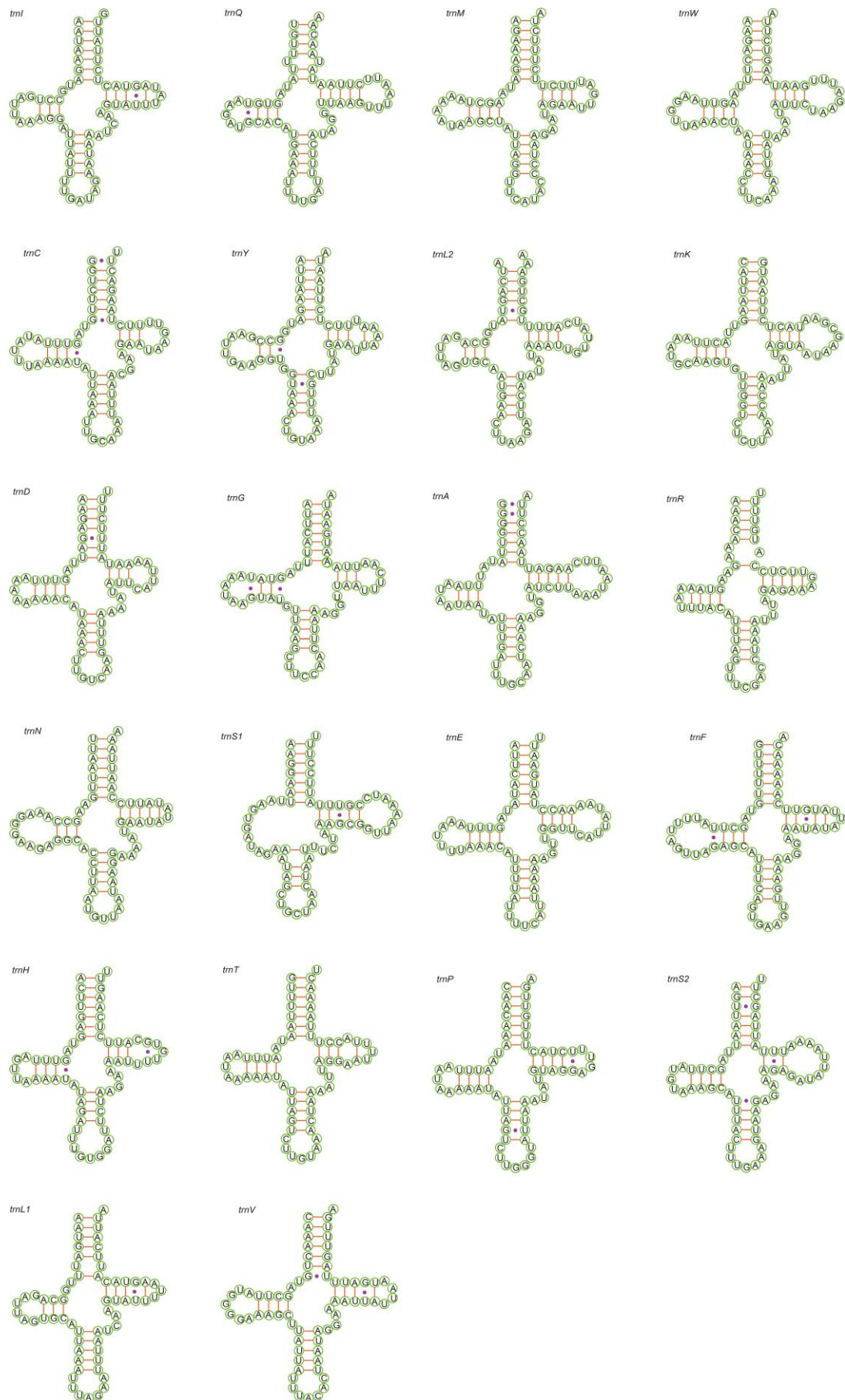


**Figure S7.** Predicted secondary structures of tRNA genes of *Doratura homophyla*.

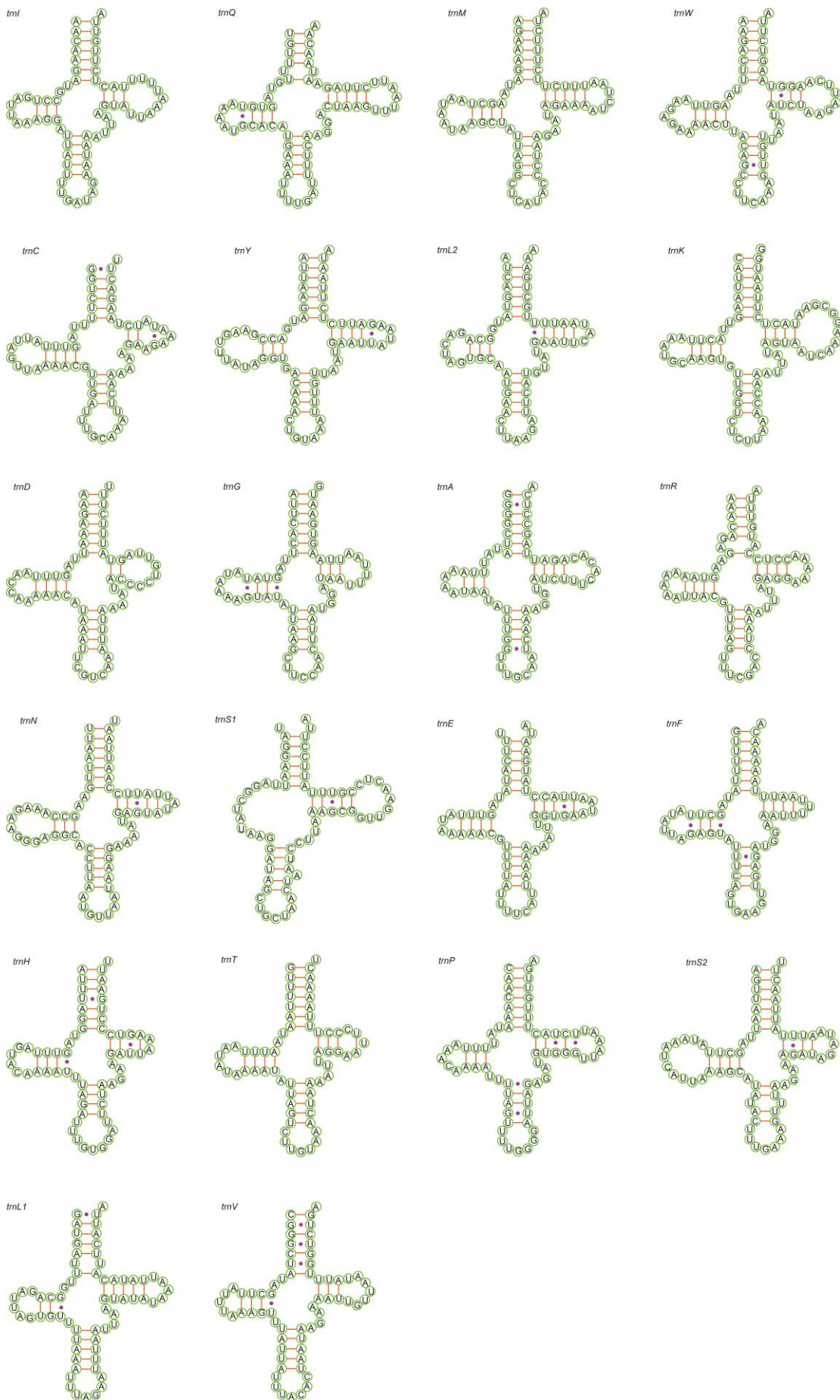


**Figure S8.** Predicted secondary structures of tRNA genes of *Gurawa minorcephala*.

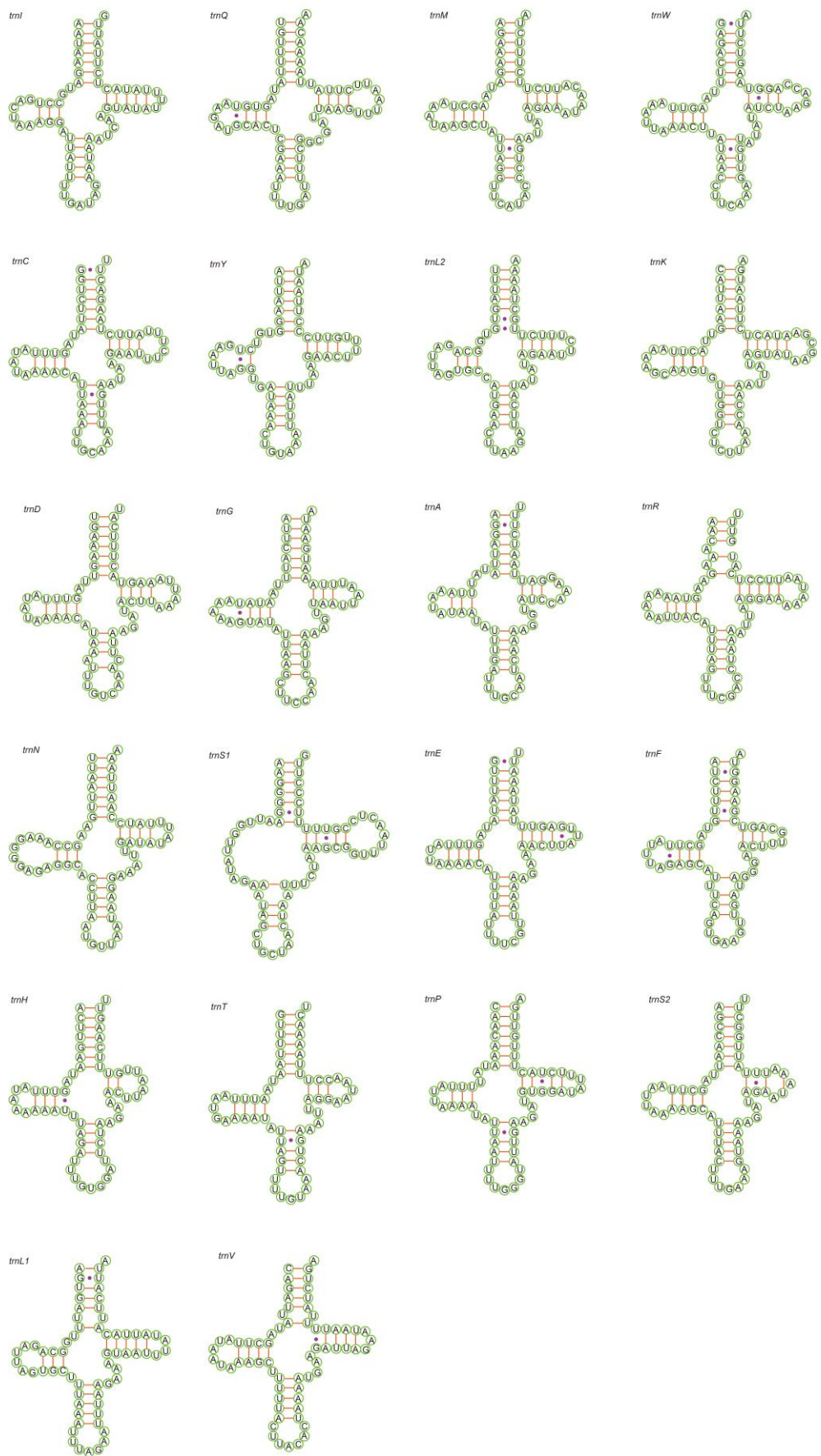


**Figure S9.** Predicted secondary structures of tRNA genes of *Leofa pulchella*.

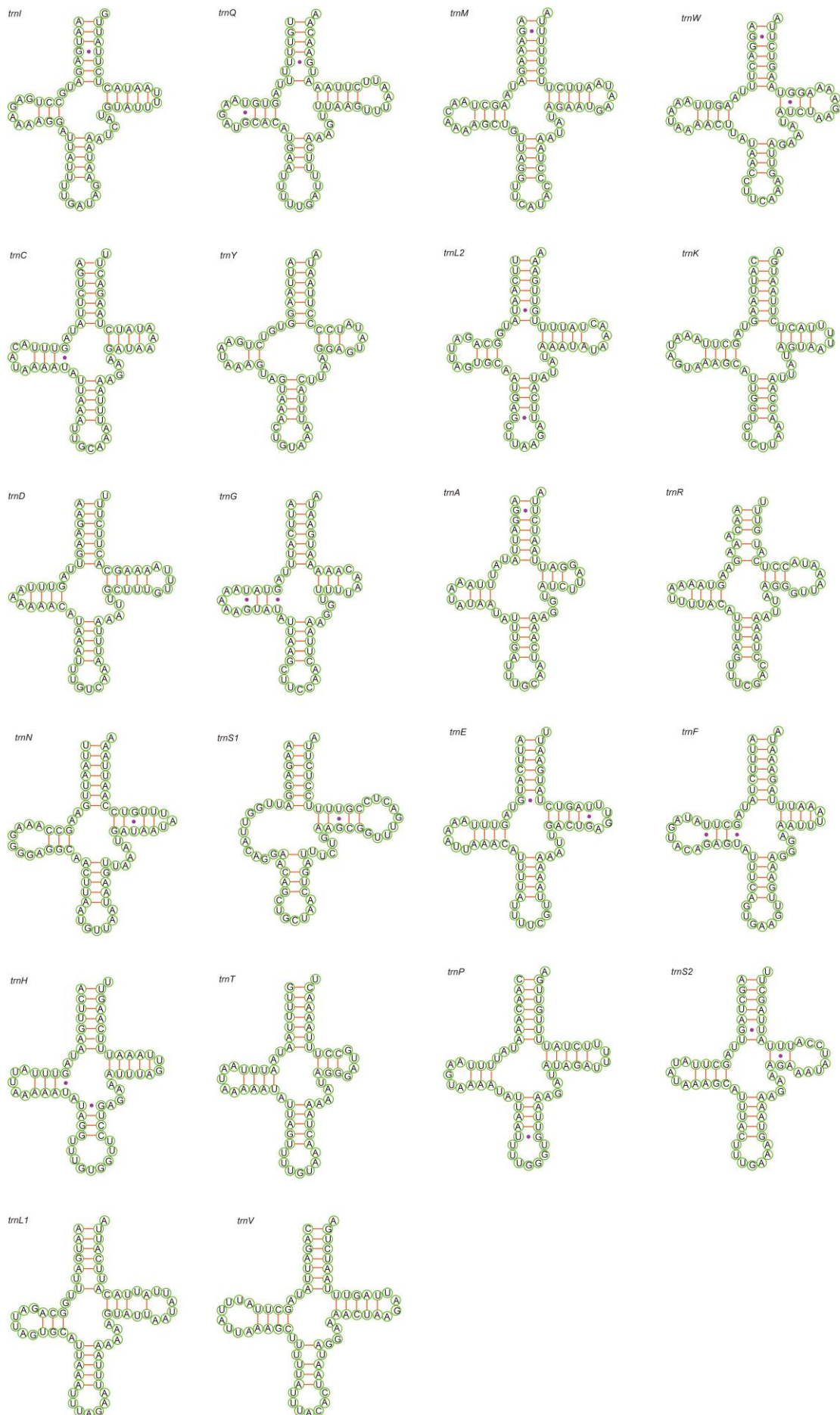


**Figure S10.** Predicted secondary structures of tRNA genes of *Nephrotettix malayanus*.

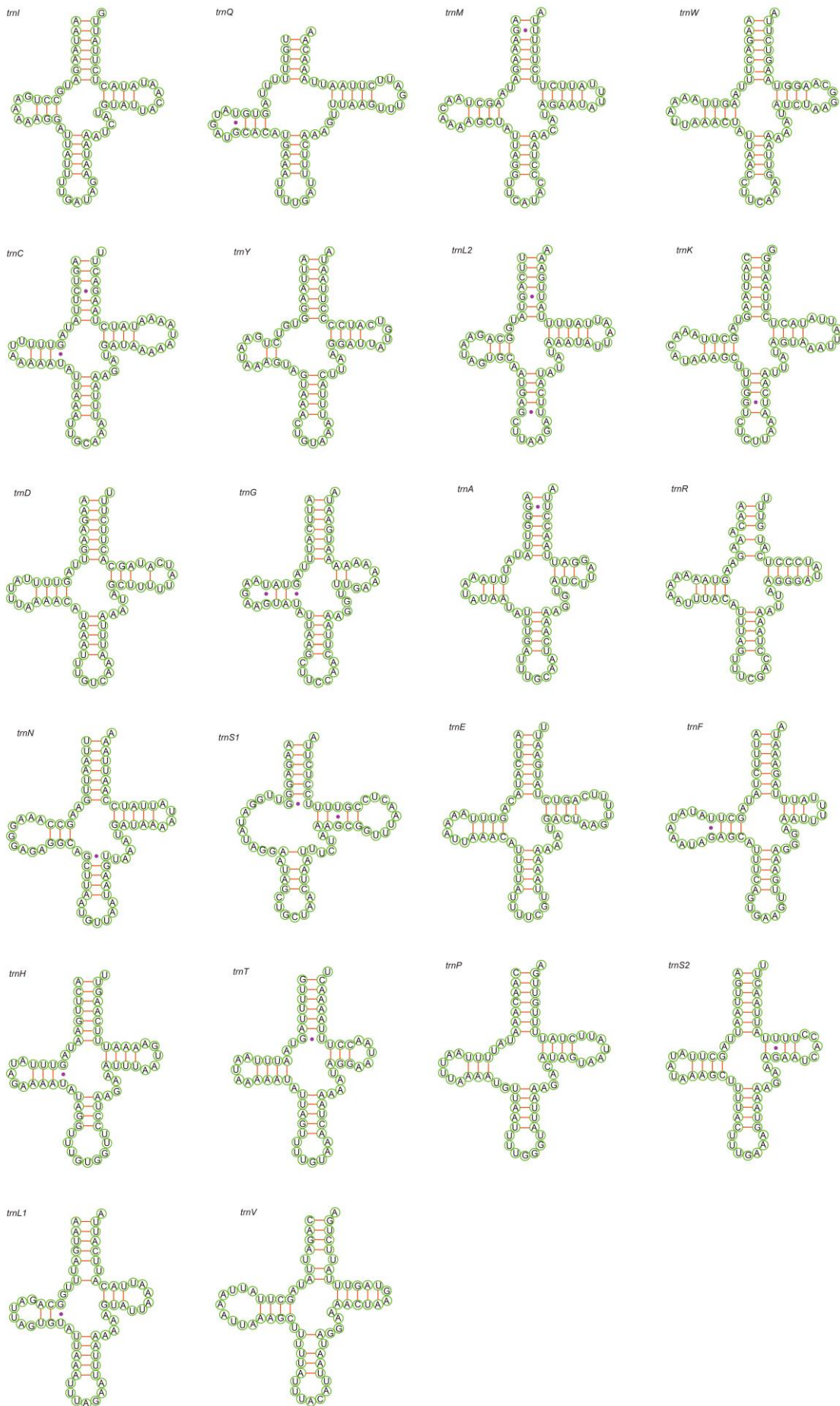


**Figure S11.** Predicted secondary structures of tRNA genes of *Nephrotettix nigropictus*.

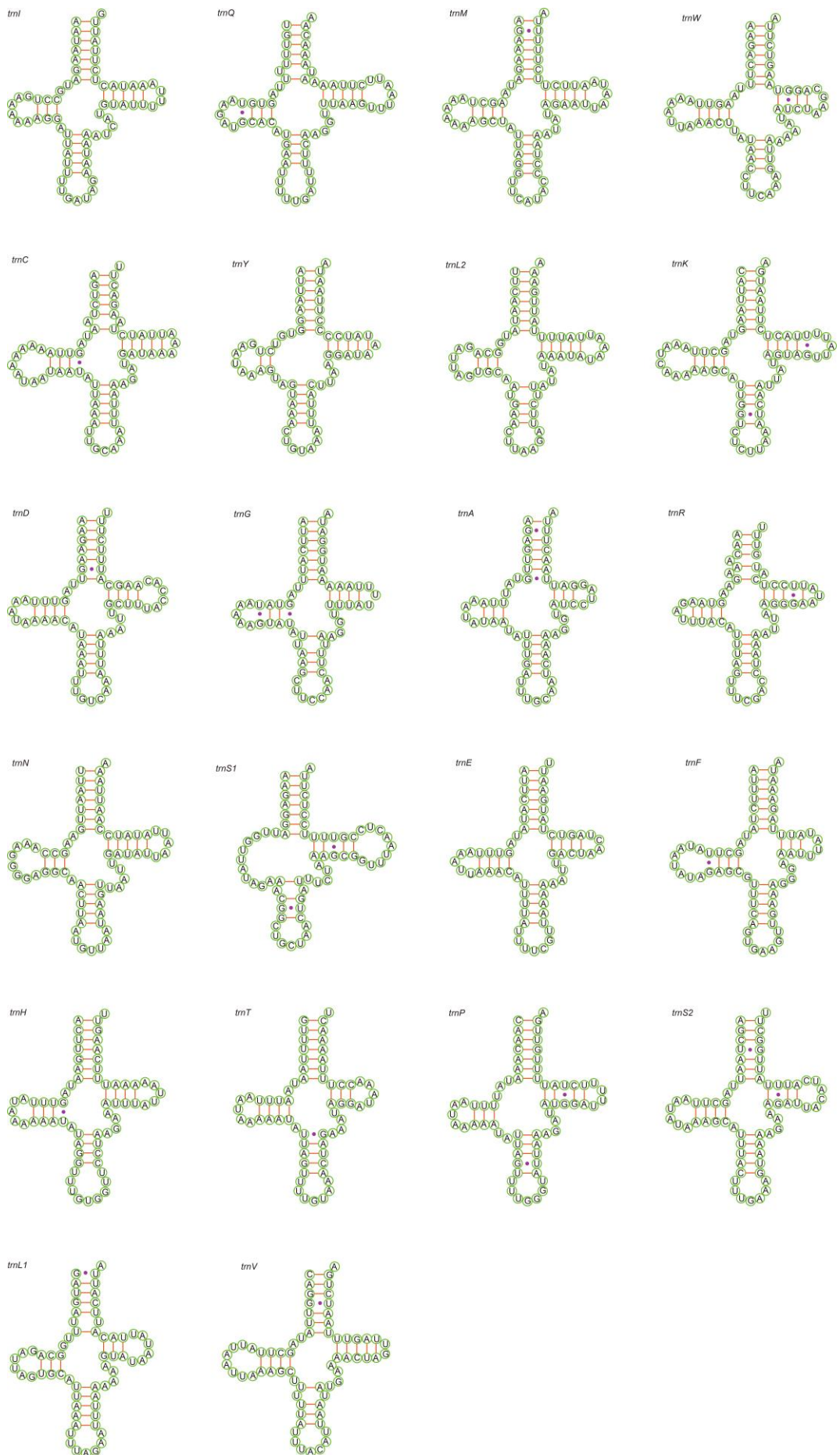


**Figure S12.** Predicted secondary structures of tRNA genes of *Nephrotettix parvus*.

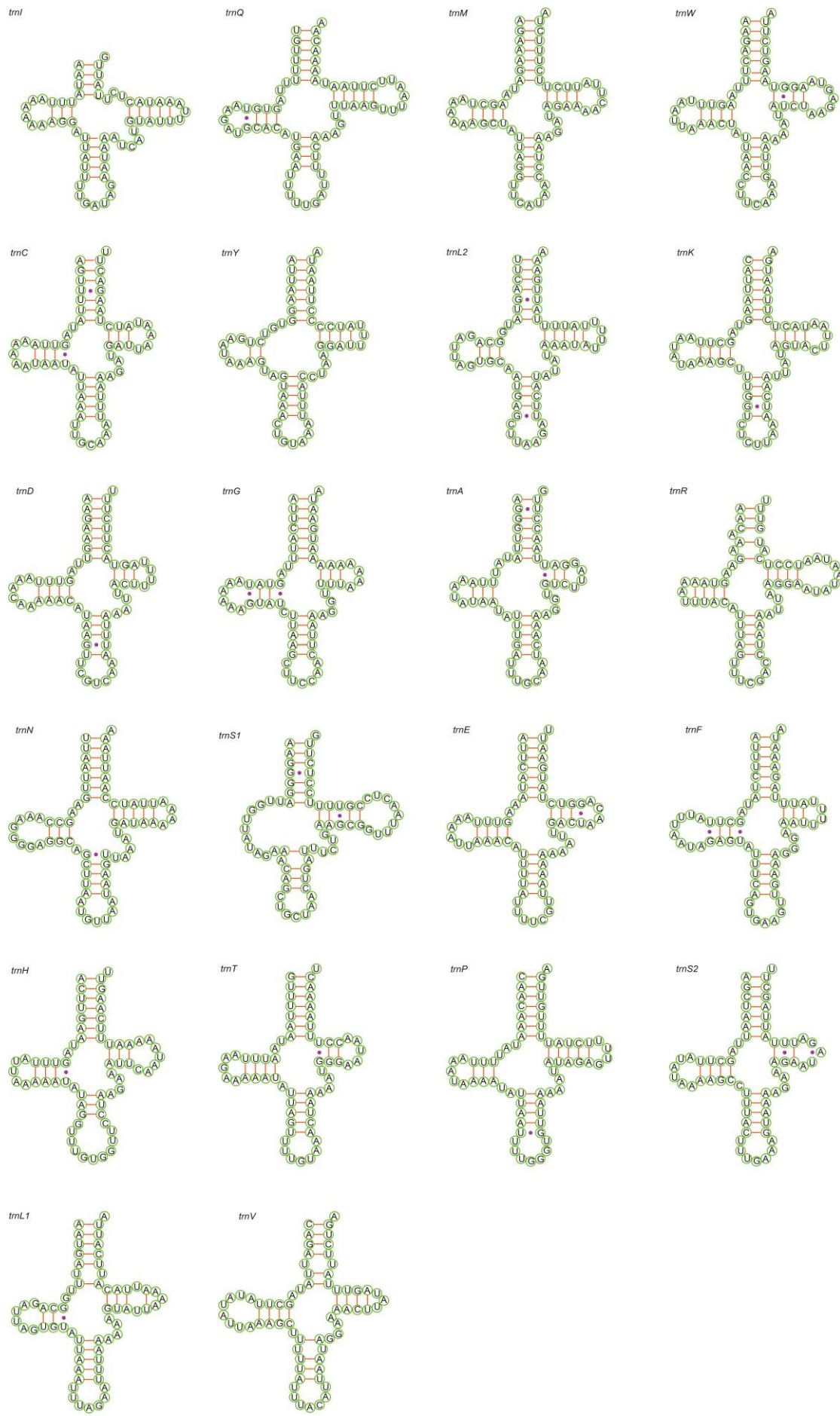


**Figure S13.** Predicted secondary structures of tRNA genes of *Nephrotettix virescens*.

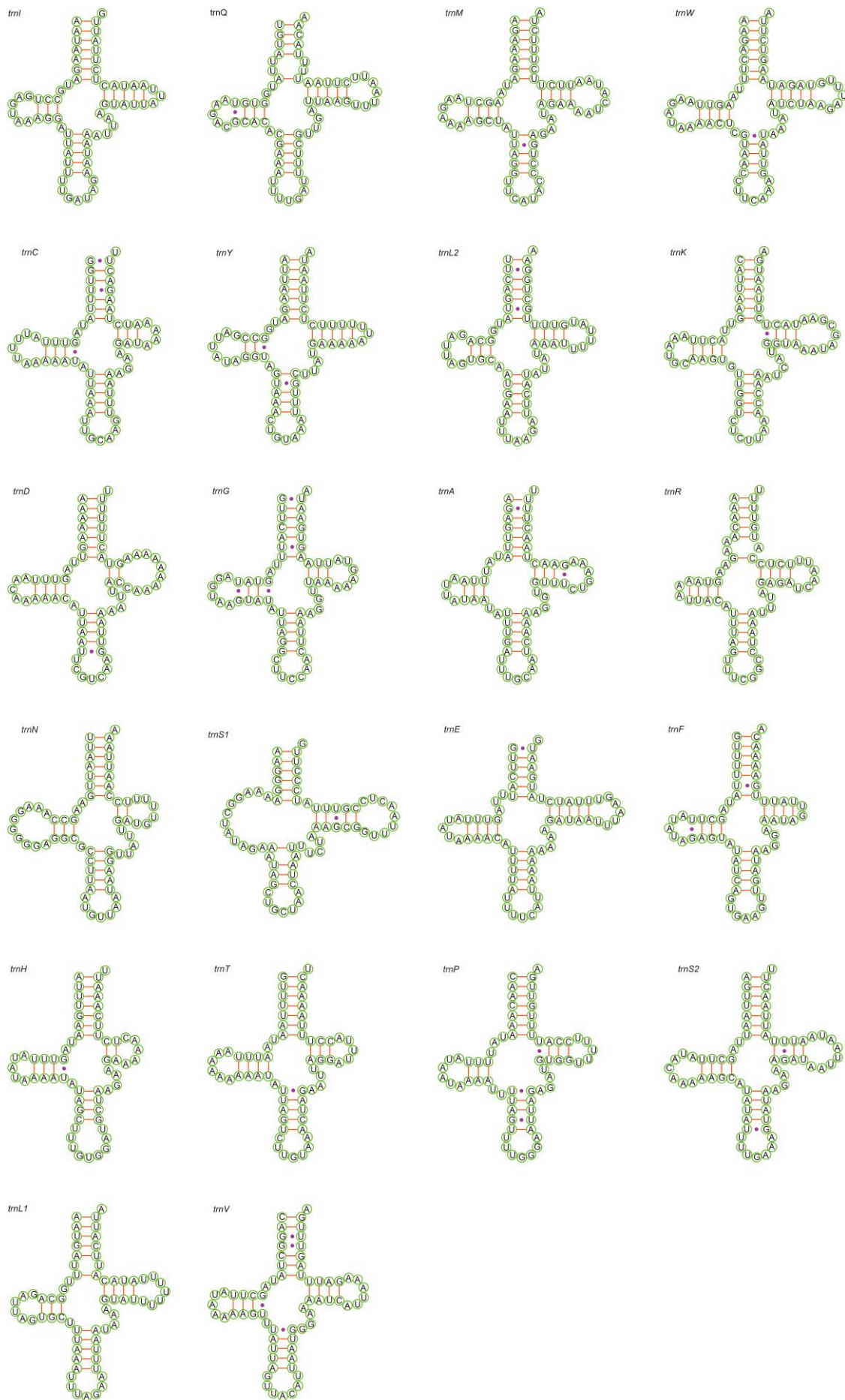


**Figure S14.** Predicted secondary structures of tRNA genes of *Zahniserius cylindricus*.

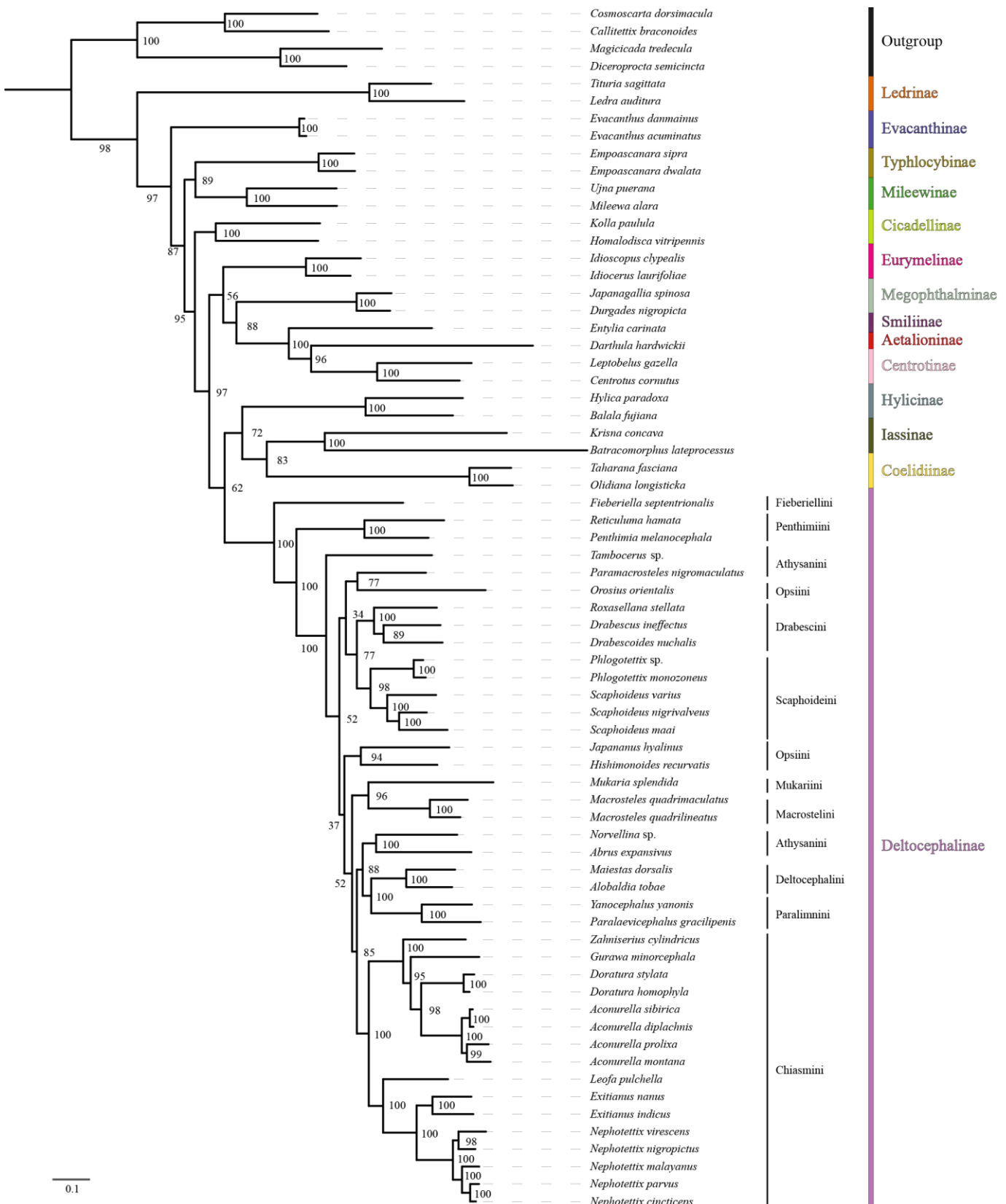


**Figure S15.** The phylogenetic relationships using the maximum likelihood (ML) analysis method based on the AA datasets. Numbers on each node correspond to the bootstrap values.

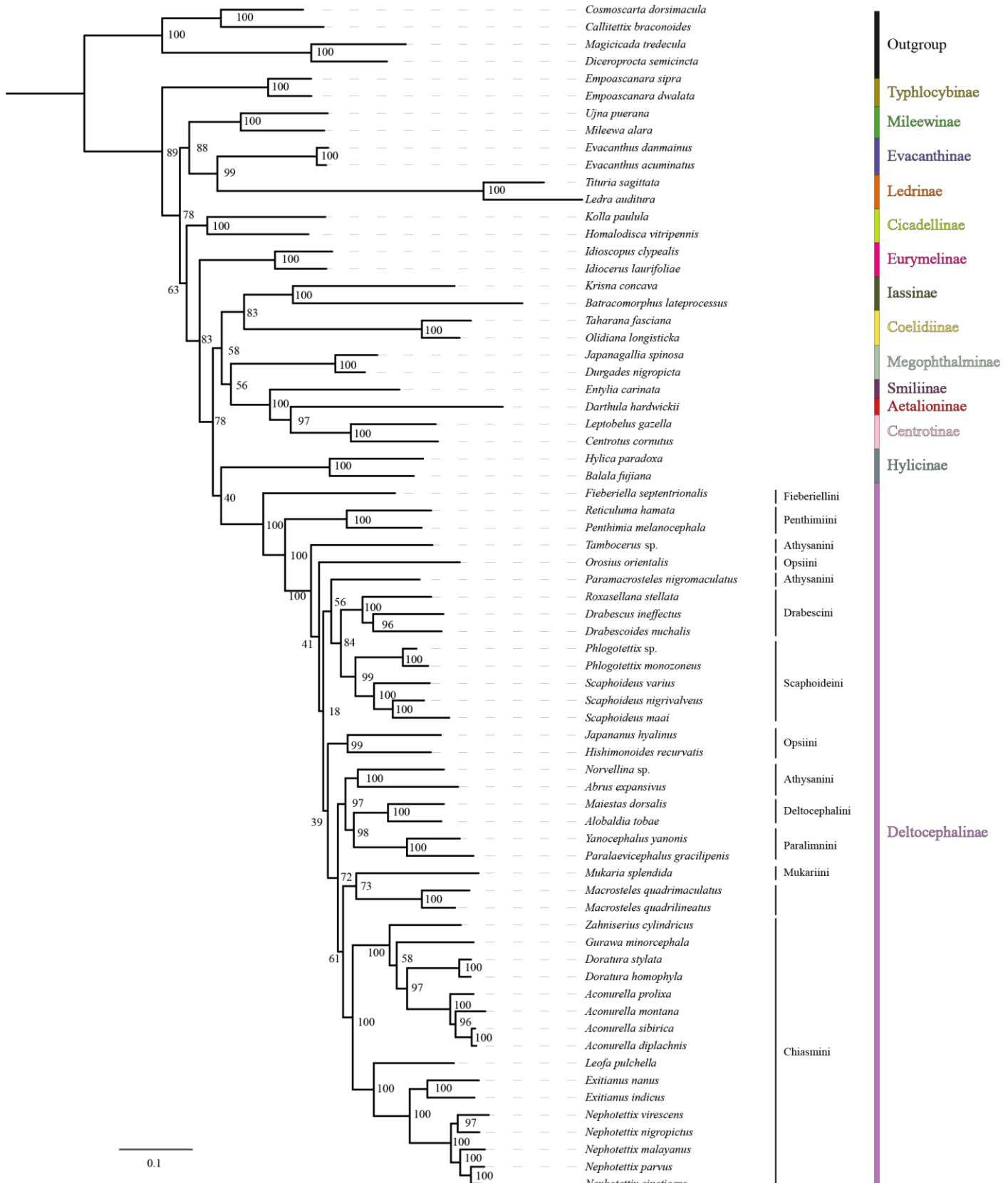


**Figure S16.** The phylogenetic relationships using the maximum likelihood (ML) analysis method based on the PCG12 datasets. Numbers on each node correspond to the bootstrap values.

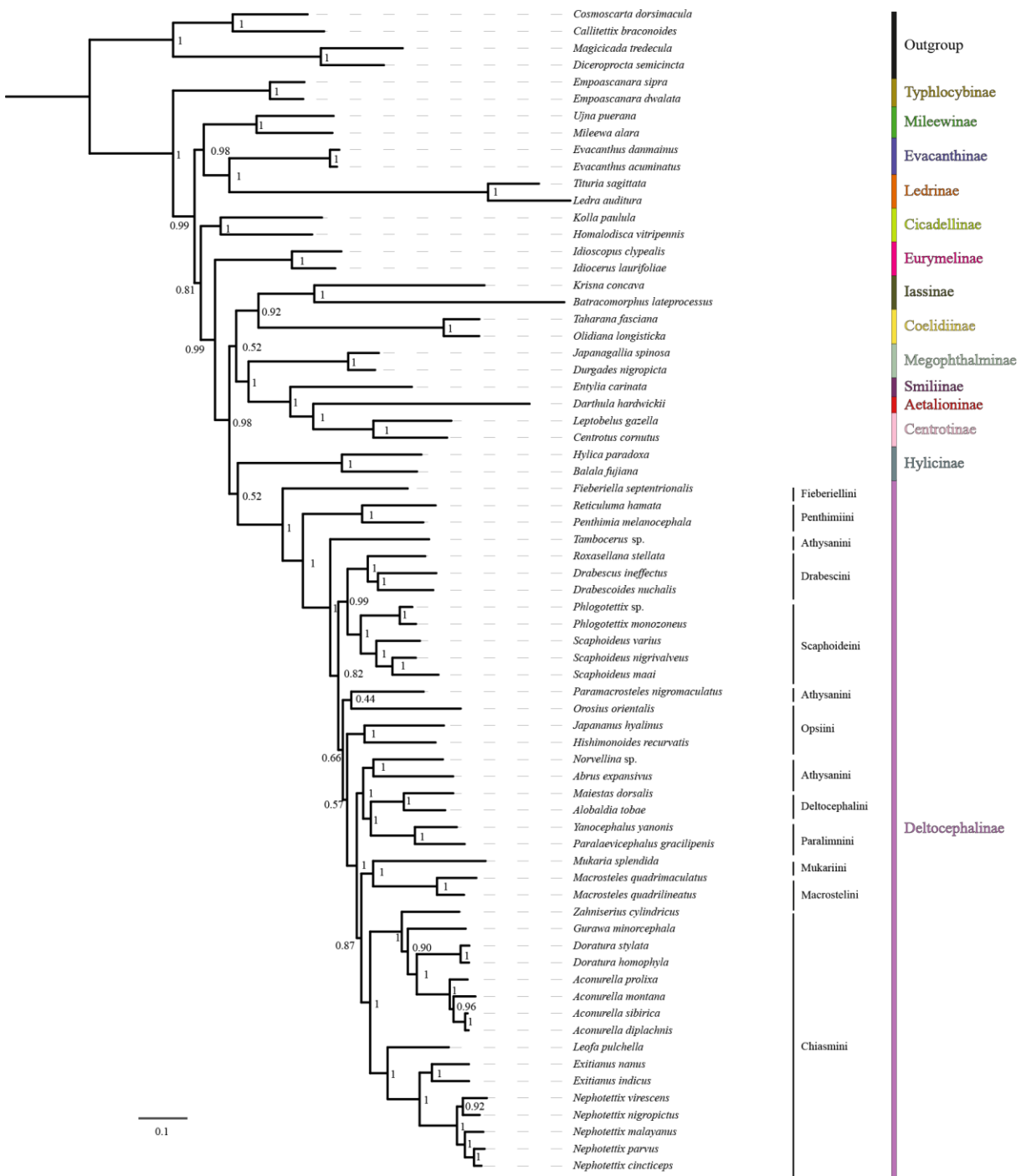


**Figure S17.** The phylogenetic relationships using the Bayesian inference (BI) analysis method based on the PCG12 datasets. Numbers on each node correspond to the posterior probability (PP) values.

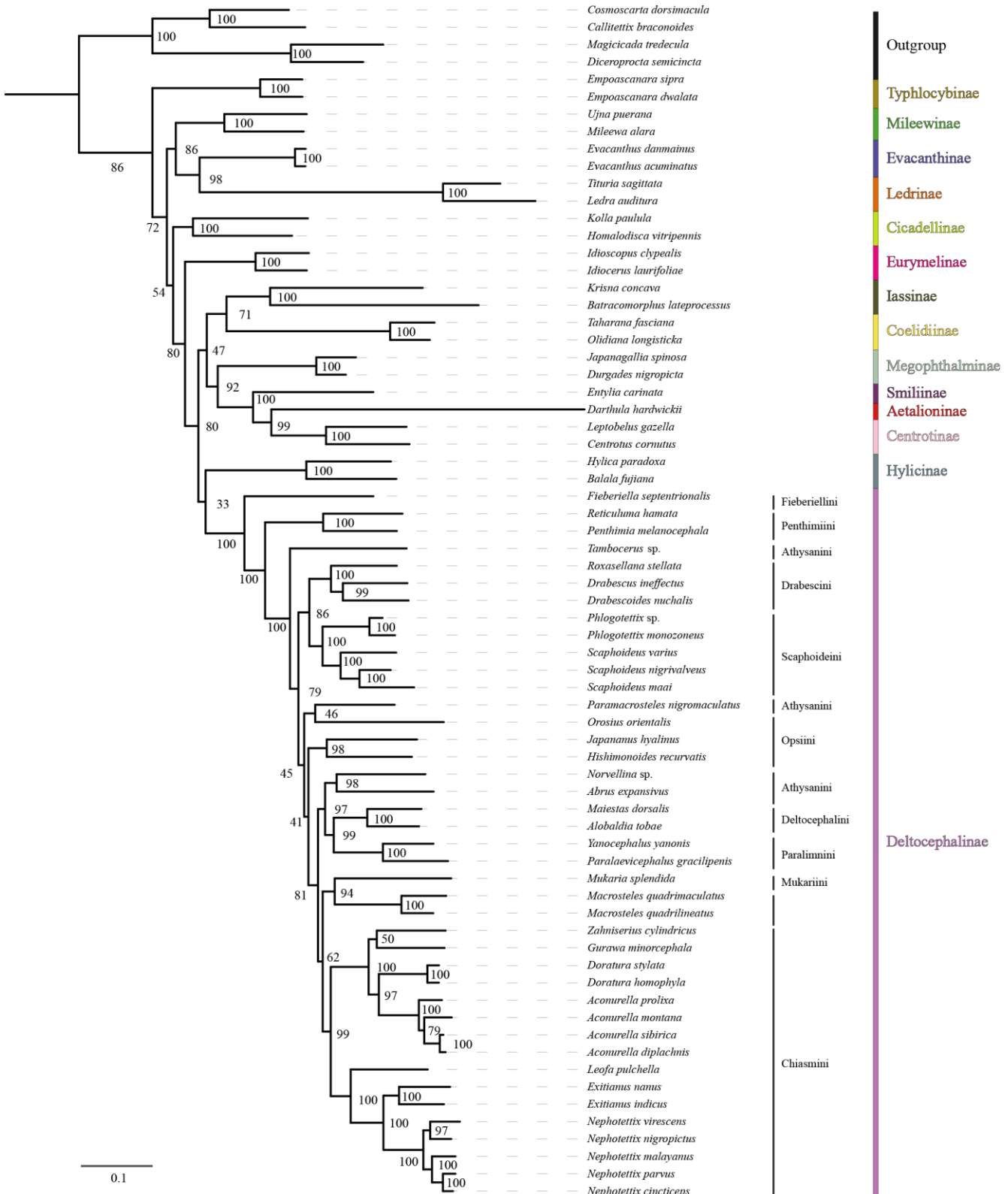


**Figure S18.** The phylogenetic relationships using the maximum likelihood (ML) analysis method based on the PCG12R datasets. Numbers on each node correspond to the bootstrap values.

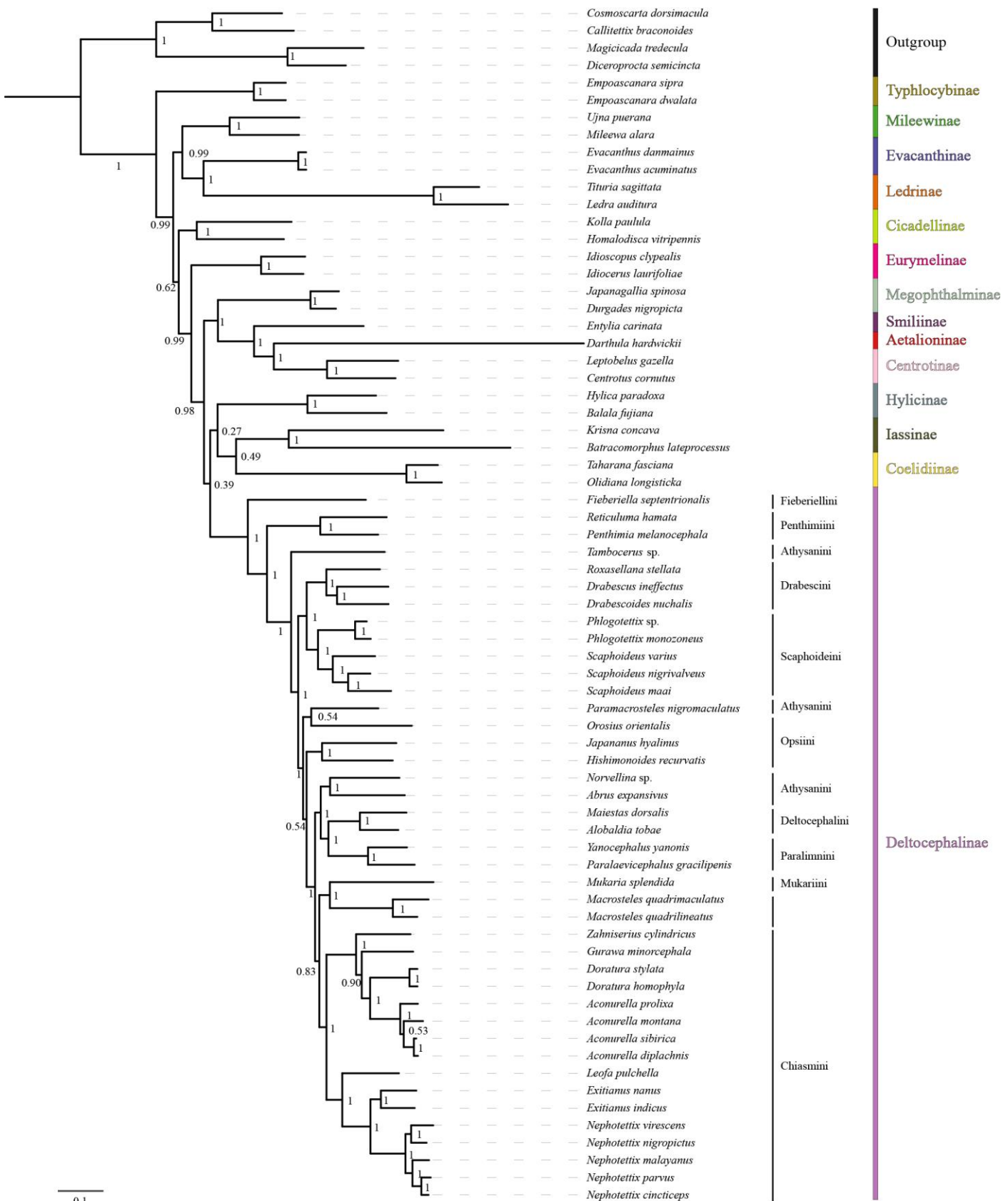


**Figure S19.** The phylogenetic relationships using the Bayesian inference (BI) analysis method based on the PCG12R datasets. Numbers on each node correspond to the posterior probability (PP) values.

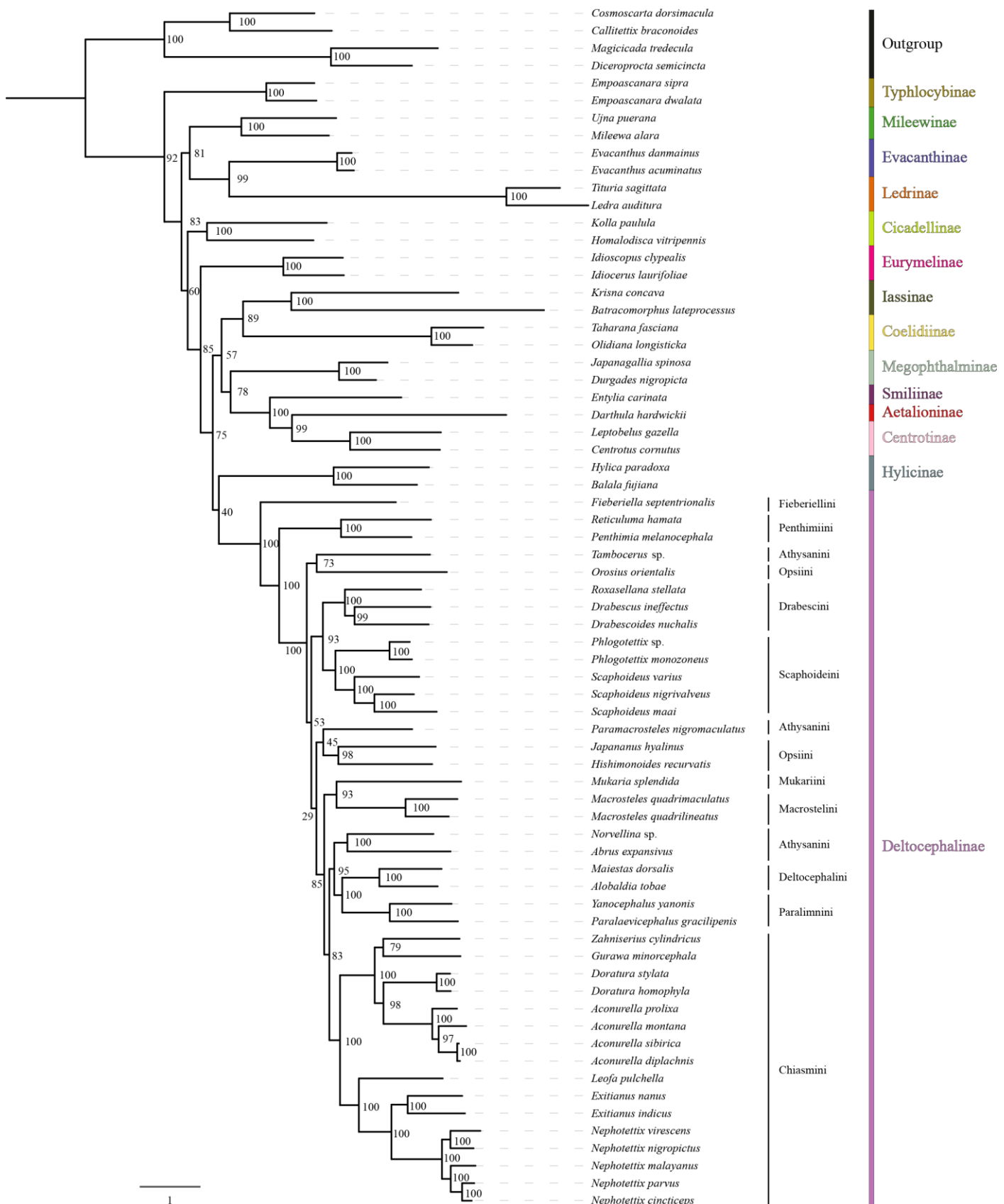


**Figure S20.** The phylogenetic relationships using the maximum likelihood (ML) analysis method based on the PCG datasets. Numbers on each node correspond to the bootstrap values.

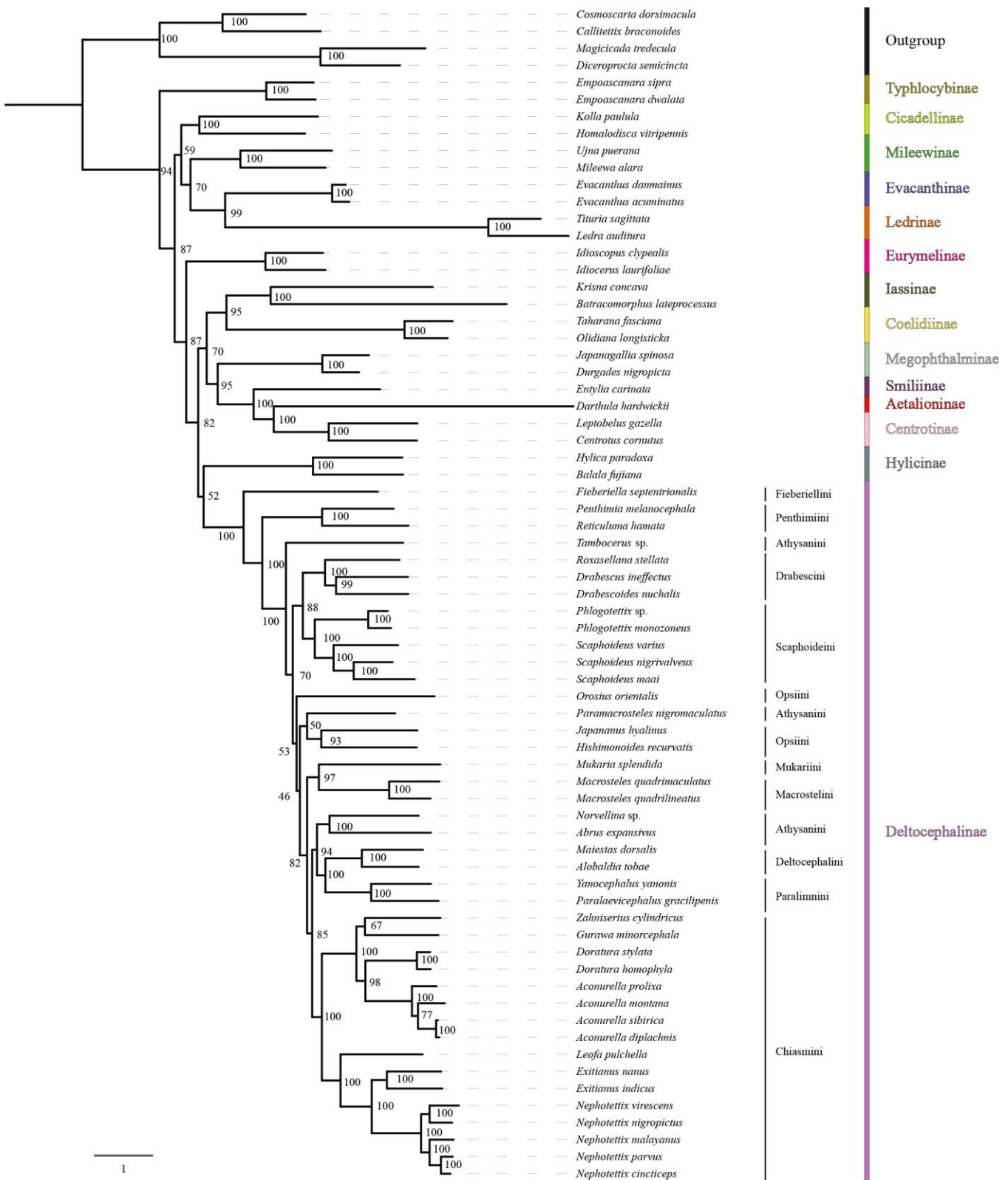


**Figure S21.** The phylogenetic relationships using the maximum likelihood (ML) analysis method based on the PCGR datasets. Numbers on each node correspond to the bootstrap values.

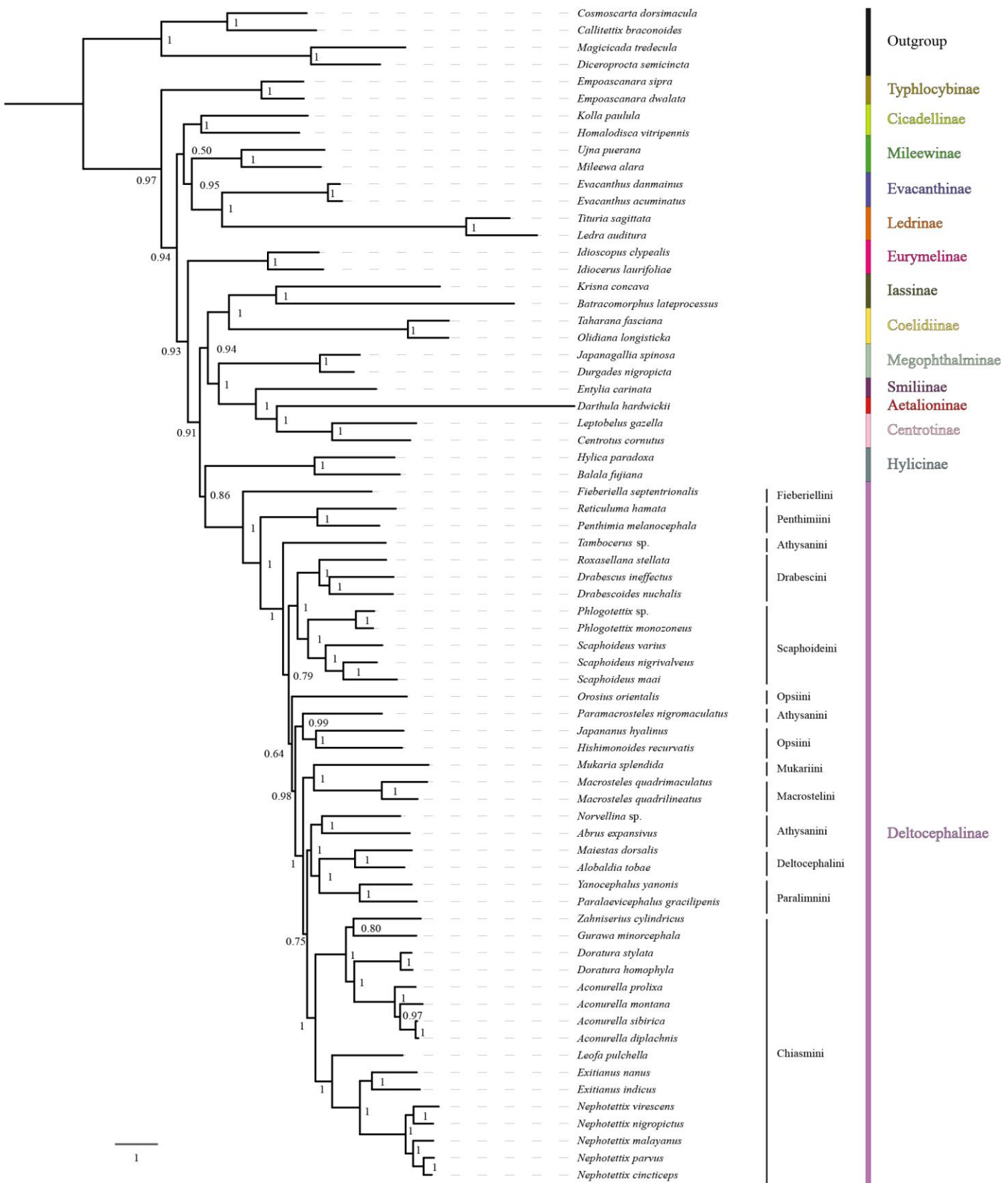


**Figure S22.** The phylogenetic relationships using the Bayesian inference (BI) analysis method based on the PCGR datasets. Numbers on each node correspond to the posterior probability (PP) values.